Journal of Operation and Automation in Power Engineering

vol. XX, no. XX, Dec. 2022, Pages: XXXX (Proofed)

http://joape.uma.ac.ir

Optimal Allocation of Renewable Energy Sources to Enhance Distribution System Reliability with Confidence Interval Considerations

M. Hajibeigy, V. Talavat, and S. Galvani*

Department of Power Engineering, Faculty of Electrical and Computer Engineering, Urmia University, Urmia, Iran.

***Abstract*—** *Due to ever-increasing energy requirements, modern distribution systems are integrated with renewable energy sources (RESs), such as wind turbines and photovoltaics. They also bring economic, environmental, and technical advantages. However, they face the network operator with decision-making challenges due to their uncertain nature. Modern distribution systems usually operate at safety margins, and any contingency may lead to power supply losses. In this regard, any attempts to increase the planner/operator's awareness of the network situation will help improve the decision quality. This paper determines the optimal locations of the RESs to enhance the expected power not served as a reliability index. Besides, it reduces power losses and minimizes the 95% confidence interval of power losses, as much as possible for having more awareness of network states. The K-medoids data clustering method is applied to handle the uncertainties of the RESs and demand loads. The MOPSO, NSGA II, and MOGWO algorithms are used to solve the proposed problem. The efficiency of the proposed approach is tested on the IEEE standard 33-bus and 118-bus distribution networks. The obtained results show that it is possible to reach a better confidence interval while keeping the losses and reliability index at a desired level. Considering solutions with identical losses and reliability index, the confidence interval of power losses using the MOPSO algorithm is 6.86% and 39.82% better rather than the NSGA II and MOGWO algorithms in the 33-bus distribution network and it is 30.23% and 129.63% better in the 118-bus distribution network.*

***Keywords*—**Optimal allocation, renewable energy sources, distribution system, confidence interval.

NOMENCLATURE

Abbreviations

2m PEM	2m point estimate method
DDP	Dual dynamic programming
DG	Distributed generation
EPNS	Expected power not served
GA	Genetic algorithm
GABC	Gbest-guided artificial bee colony
GWO	Grey wolf optimizer
MCS	Monte carlo simulation
MILP	Mixed-integer linear programming
MOGWO	Multi-objective grey wolf optimizer
MOPSO	Multi-objective particle swarm optimization
MOWO	Multi-objective whale optimization
NSGA II	Non-dominated sorting genetic algorithm
P-OPF	Probabilistic optimal power flow
PDF	Probability density function
PNS	Power not served
PSO	Particle swarm optimization
PV	Photovoltaic
RES	Renewable energy source
SCA	Sine cosine algorithm
SSA	Salp swarm algorithm
TOPSIS	Technique for order of preference by similarity to the ideal solution
UPFC	Unified power flow controller
WT	Wind turbine

Received: 07 Dec. 2023
Revised: 30 Jan. 2024
Accepted: 13 Feb. 2024
*Corresponding author:
E-mail: v.talavat@urmia.ac.ir (V. Talavat)
DOI: 10.22098/joape.2024.14178.2087
Research Paper

1. INTRODUCTION

1.1. Motivation

RESs play an essential role in solving environmental problems and promoting sustainable improvement worldwide. They also have advantages such as modifying the distribution network power losses, postponing the system upgrade, and enhancing the voltage profile. However, these systems suffer from voltage fluctuations due to their intermittency and the fact that voltage exceeds the upper limitations due to the higher RES production or lower load. The optimal power flow model of a distribution network with RES supply and the optimal programming model of a regular distribution network have significantly changed in terms of optimization objectives, optimization methods, selection of system constraints, and control variables. The effectiveness of RESs depends on their siting in the distribution networks [1]. Furthermore, the main goal of power companies is to provide reliable and sustainable energy to their customers, so it is essential to establish criteria for evaluating distribution networks for continuous energy supply [2, 3]. In this context, a reliable method should be applied to determine the size and location of RESs. The stochastic nature of RESs and their significant penetration into the distribution network presents technical challenges regarding the system's operation. Thus, integrating RESs into distribution networks increases the complexity of the analysis that must be conducted to make accurate and efficient decisions regarding network operation [4].

Furthermore, large-scale RES penetration in distribution networks increases the risks to the economic and secure function of the distribution network. To overcome this problem, a robust optimization method based on a confidence interval index can effectively guarantee the optimal operation of a distribution network in the random fluctuation environment of RESs and loads [5].

1.2. Literature review

Paper [6] addresses the optimal sizing and allocation of DGs for power losses, voltage profile, and stability improvement, introducing a stability index based on Thevenin impedance in a distribution network. Study [7] reduces power losses and yearly economic loss in a multi-objective framework with optimally sized DGs in optimal locations. Study [8] optimizes the architecture of a WT farm, including its location, height, and shadow reduction using the PSO algorithm. Paper [9] proposes an efficient optimization approach to allocate the DG units in distribution networks to improve the voltage profile, reduce power losses, and enhance the voltage stability index. In papers [6], [7], [8], and [9], the reliability of the distribution networks is not studied. In [10], several common techniques are utilized to reduce technical losses and enhance the network's reliability, such as reactive compensation, network reconfiguration, and placement of voltage regulators. This paper does not use RES allocation to improve the network's reliability. A combined scheme is presented in [11] to solve the optimal placement of RESs and assess the reliability of distribution networks. The objective functions are a reduction in power loss and an improvement in voltage stability. Paper [12] presents an optimal and simultaneous allocation of the PV and WT with the reconfiguration of radial distribution networks to decrease power loss cost and improve reliability. Papers [6], [7], [8], and [12] do not consider network uncertainties. Paper [13] uses a probabilistic approach to explore the influence of a unified power flow controller on enhancing power system reliability and improving its operation under normal operating conditions. Paper [14] presents a method to integrate expected power not supplied and the loss of load probability constraints in the power systems expansion planning problem. Probabilistic analyses are applied in the corresponding studies, but the siting of the RESs is not applied. The confidence interval index, as a key parameter in this paper, is not considered in any of the cited studies. Despite numerous studies addressing the optimal probabilistic power flow problem, there remains a dearth of research exploring using probabilistic approaches to account for uncertainties and assess the probability of technical issues arising during intermittent generation optimization. Existing studies either presuppose a normal distribution for output state variables or rely solely on the expected values, potentially resulting in an inaccurate depiction of the actual behavior of objective variables [15–17]. A confidence interval estimation method may also provide the optimal solution when operating in an uncertain environment. Based on the probabilistic power flow evaluation, [18] proposes a probabilistic optimization algorithm for dealing with the probability of overvoltage occurrence when harvesting the maximum PV generation while keeping the system voltage within acceptable confidence levels. Paper [19] proposes a novel multi-objective distributed generation planning methodology in distribution networks considering correlations among uncertainties with the objective functions of minimizing both the annual total cost and the risk. Besides, the confidence interval concept is used to specify the constraint-allowed levels. The reliability of the studied system is not considered in papers [18] and [19]. Table 1 provides a more detailed comparison of the existing studies and the current study.

Although the MCS can represent complex systems, it is a computationally intensive method that requires high computational effort to reach acceptable values; as a result, it plays a minor role in practical applications. The K-medoids algorithm is used to estimate the statistical information of variables by using representative scenarios. It is a powerful method that approximates statistical information accurately. Consequently, this technique presents a reasonable and efficient computational effort suitable for practical applications [20].

1.3. Paper contribution

The key contribution of this study is considering the confidence interval as an objective besides conventional objectives such as losses and reliability index, in the optimal allocation of RESs problem. This will lead to choosing solutions that not only satisfy the losses and reliability criteria but also decrease the confidence interval to have more awareness of the network state.

Also, some other key features of this paper are as follows:

- Implementing different optimization algorithms, i.e., MOPSO, NSGA II, and MOGWO, to solve the problem and compare the results
- Probabilistic evaluation of the problem using the K-medoids method
- Employing the multi-criteria decision-making TOPSIS technique to select final solutions

2. PROBABILISTIC OPTIMAL POWER FLOW

Optimal power flow with renewable generation sources has become a common tool utilized in the power system operation planning and electricity market. A vital problem in optimal power flow is considering an appropriate model for system uncertainties that may cause an outage or even collapse. In this condition, P-OPF can decrease the risk of outages. A comprehensive P-OPF method is crucial to formulate modern power systems that include some additional constraints on voltage stability problems of wind power, solar power, and demand load. This method extensively assesses the system's overall status due to using a set of input parameters to calculate the output rather than just one specific operating point [21].

Generally, there are three primary categories for probabilistic evaluation in P-OPF: MCS, approximate, and analytical methods. While the MCS approach is highly accurate and adaptable to various problems, it requires additional computational effort. In contrast, other techniques provide quicker results due to simplified modeling but sacrifice precision. Therefore, a trade-off must be established between the accuracy and speed of computation. As a solution, the K-medoids method, proposed by Michael McKay in 1979, serves as a sampling approach to reduce the number of MCS representatives while still maintaining a nearly precise assessment capability [22]. The description and formulation of the K-medoids method are presented in Subsection 2.2.

2.1. Uncertain input variables

Probability density functions are used in P-OPF to describe the input variables. Considering the precise analytical model to estimate the uncertain input variables is essential. As a result, wind speed, solar radiation, and power demand can be modeled in a PDF form as follows: WTs depend on wind speed to generate electricity. Various distribution models have been employed to model wind speed, including gamma, Rayleigh, lognormal, Burr, Nakagami, generalized extreme value, inverse Gaussian, Gumbel, and Weibull. The Weibull distribution is commonly applied to model wind speed. Thus, the Weibull distribution is employed in this paper. The PDF of the Weibull distribution is represented as Eq. (1) [23].

$$f(v) = \begin{cases} \left\{\frac{k}{\lambda}\left(\frac{v}{\lambda}\right)^{k-1} \times e^{-\left(\frac{v}{\lambda}\right)^{k}} \quad v \geq 0 \\ 0 v < 0 \end{cases} \tag{1}$$

Table 1. Comparison of references with the current study.

Reference	Optimization algorithm	Objective function	Probabilistic method	RES allocation	Reliability	Power losses	Uncertainty	Confidence interval
[6]	GWO GA	Power losses Voltage profile Stability index	-	√	×	√	×	×
[7]	MOWO	Power losses Yearly economic loss	-	√	×	√	×	×
[8]	PSO	Energy output	-	√	×	×	×	×
[9]	SCA	Voltage stability index Power losses Voltage profile	Chaotic map	√	×	√	√	×
[10]	MILP	Power losses Voltage profile Reliability index	-	×	√	√	×	×
[11]	GABC	Power loss Voltage stability index Voltage level	-	√	√	√	×	×
[12]	SSA	Power losses cost Reliability	-	√	√	√	×	×
[13]	PSO	EPNS Active power losses Voltage deviation Cost of power generation and UPFC allocation	2m PEM LHS	×	√	√	√	×
[14]	DDP	Loss of load probability Voltage stability index Voltage level	MCS	×	√	√	√	×
[18]	Probabilistic algorithm-based 2m+1 PEM Edgeworth	Overvoltage occurrence	2m+1 PEM	×	×	×	√	√
[19]	NSGA II	Annual total cost Risk	MCS	×	×	×	√	√
This paper	MOPSO NSGA II MOGWO	EPNS Power losses CI of the power losses	K-medoids	√	√	√	√	√

where k and λ are the shape and scale parameters, and v is the wind speed. The following equation can determine wind turbine generation:

$$P_{WT}(v) = \begin{cases} 0 & v \le v^{cut-in} \text{ or } v \ge v^{cut-out} \\ \frac{v - v^{cut-in}}{v^{rated} - v^{cut-in}} \times P_{WT}^{rated} & v^{cut-in} \le v \le v^{rated} \\ P_{WT}^{rated} & v^{rated} \le v \le v^{cut-out} \end{cases} \quad (2)$$

where

v^{cut-in} and $v^{cut-out}$ are the WT cut-in and cut-out speeds, respectively;

v^{rated} is the rated speed of the WT;

P_{WT}^{rated} is the rated output power of the WT.

Similarly, PV generation relies on solar radiation. The beta distribution is commonly used to predict solar radiation. The PDF of the beta distribution is represented as Eq. (3) [24].

$$f(r) = \frac{\Gamma(\alpha+\beta)}{\Gamma(\alpha)\Gamma(\beta)} \times r^{\alpha-1}(1-r)^{\beta} \quad (3)$$

where α and β are the beta distribution shape parameters, and r is the solar radiation.

PV generation can be determined by the following equation:

$$P_{PV}(r) = \begin{cases} P_{PV}^{rated} \times \left(\frac{r^2}{r^{std} r^{cer}}\right) & 0 \le r < r^{cer} \\ P_{PV}^{rated} \times \frac{r}{r^{STD}} & r^{cer} \le r < r^{std} \\ P_{PV}^{rated} & r^{std} \le r \end{cases} \quad (4)$$

where

r^{cer} is a radiation at certain point;

r^{std} is the solar radiation in standard conditions;

P_{PV}^{rated} is the rated output power of the PV cell.

In previous studies, several distribution models, such as Weibull, Rayleigh, and normal, have been utilized to model the demand load [25]. The normal distribution is selected in this paper. The PDF of the normal distribution is expressed as Eq. (5) [26].

$$f(P_L) = \frac{1}{(\sigma[P_L])\sqrt{2\pi}} \times e^{-\frac{(P_L - E[P_L])^2}{2\sigma[P_L]^2}} \quad (5)$$

where $\sigma[]$ and $E[]$ are the standard deviation and expected value operators, respectively.

2.2. Describing the K-medoids data clustering method

Data clustering was first introduced in 1935 to separate large, multidimensional objects or data into subsets called clusters. In this process, objects or data within a cluster are generally more similar to each other than those in other clusters using a specific criterion, such as distance. This method allows a limited number of datasets to be analyzed instead of processing a large volume of information.

K-means [27] and K-medoids [28] are clustering-based methods that partition a set of data points into clusters, with a minimum sum of the distances between the data points and the agent of their clusters. Nevertheless, there are some critical differences between these algorithms:

- Cluster agent: In K-means, the mean of the data points in the cluster is used as a cluster agent. In K-medoids, the agent of a cluster known as medoid is an actual data point in the cluster.
- Computational burden: Computing the mean value of a cluster is more simple than finding the medoid. Thus, the K-means method is usually faster than the K-medoids method.
- Outlier vulnerability: In K-means, the cluster agent is sensitive to outlier points. These outline points can significantly affect the mean value of a cluster. However, the K-medoids method is more resistant to outliers since the medoids are less influenced by outline points.

The K-means is a widely used method, but the K-medoids show a more acceptable level of accuracy in estimating lower-order

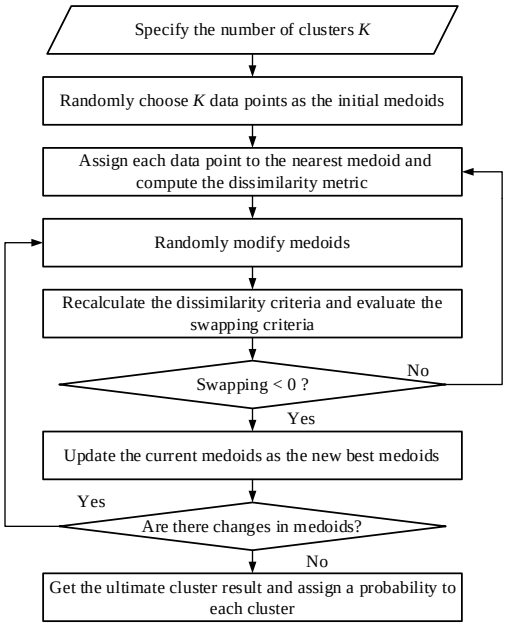

Fig. 1. The flowchart of the k-medoids method.

statistical moments of output variables. The flowchart of the K-medoids method is presented in Fig. 1.

K-medoids can be implemented as follows:

Step 1: Specify the number of clusters (K).

Step 2: Select initial medoids for N random input variables.

2.1) Using the Euclidean distance as a measure of dissimilarity, calculate the distance between every pair of data points in the following manner:

$$d_{ij} = \sqrt{\sum_{n=1}^{N} (x_{in} - x_{jn})^2} \; . \; i.j = [1.\ 2.\ \ldots.\ S] \tag{6}$$

where

d_{ij} is the distance between every pair of data points;

x_{in} and x_{jn} are respectively the i and j data of the random input variable n;

S is the total number of data in each random input variable.

2.2) To make an initial estimation of the cluster centers, calculate p_{ij} as follows:

$$p_{ij} = \frac{d_{ij}}{\sum_{l=1}^{S} d_{il}} . \; i.j = [1.\ 2.\ \ldots.\ S] \tag{7}$$

2.3) Compute $\sum_{i=1}^{S} p_{ij}$ $(j = [1.\ 2.\ \ldots.\ S])$ for each data point and arrange them in ascending order. Then, select k data point with the smallest value as the initial medoids for the cluster.

2.4) Allocate each data point to its closest medoid.

2.5) Compute the present optimal value, which is the summation of the distances between all objects and their respective medoids.

Step 3: Update medoids

Substitute the current medoid within each cluster with the data point with a minimum total distance from the other data points in the cluster.

Step 4: New allocation

4.1) Allocate each data point to the closest new medoid.

4.2) Calculate the sum of distances from all objects to their respective medoids to obtain a new optimal value. If this new optimal value equals the previous value, the medoids have stabilized, and the algorithm should be terminated. On the other hand, if the new optimal value differs from the previous value, the algorithm should go back to Step 3 and reassign objects to new medoids until the optimal value converges.

Finally, the algorithm has determined the K medoids for N random input variables $(X_k = [X_{k1}.X_{k2}.\ \ldots\ .X_{kN}].\ k = [1.\ 2.\ \ldots\ .\ K])$. This final output represents the clusters that can now be utilized for further analysis.

Moreover, the probability of each cluster is computed by Eq. (8).

$$P(X_k) = \frac{N_{G_k}}{S} . \; k = [1.\ 2.\ \ldots\ .\ K] \tag{8}$$

where N_{G_k} is the number of data points in the ${G_k}^{th}$ cluster. Besides, the i^{th} statistical moment of F is computed as Eq. (9).

$$E\left[F^i\right] = \sum_{k=1}^{K} P(X_k) \bullet F(X_k)^i \tag{9}$$

where $F(X_k)^i$ is the k^{th} output variable based on sample X_k.

3. MULTI-OBJECTIVE OPTIMIZATION PROBLEM

A multi-objective optimization problem can be defined as minimizing or maximizing certain factors $F(x) = \{f_1(x) \ldots . f_N(x)\}$, where x is the vector of M-dimensional decision variables $x = \{x_1 \ldots . x_M\}$ from some universe. A MOP can be formulated with the following equations:

$$f_n(x) .\ n = 1.2. \ldots . N \tag{10}$$

$$\text{subject to}\, g_j(x) \leq 0 \; .j = 1.2.\ \ldots\ .J \tag{11}$$

$$h_k(x) = 0.\ k = 1.2.\ \ldots\ .K \tag{12}$$

$$x_i^L \leq x_i \leq x_i^U \; . \; i = 1.2. \ldots . 1.2.\ \ldots\ .M \tag{13}$$

The objective functions are defined in Eq. (10), and Eqs. (11) and (12) state the equality and inequality constraints. A control variable is identified by the index x. In Eq. (13), the variable limits are set so that each control variable can have a value within a lower (x_i^L) and an upper (x_i^U) limit.

In multi-objective problems, the conflicting objectives can make finding a single optimal solution challenging. Instead, a set of compromised solutions, known as Pareto solutions, is obtained. This means there is no single best solution, and a range of optimal solutions are obtained [29].

There are two main approaches to optimization: mathematical and evolutionary approaches. Mathematical methods have limitations when dealing with non-convex problems, and the final solution can be influenced by the initial solution, potentially leading to entrapment in a suboptimal solution.

Evolutionary algorithms were introduced to address these limitations. They can avoid entrapment in local optimal solutions by considering a population of feasible solutions. Additionally, they do not require derivatives of the objective functions, allowing them to solve various types of problems. Despite these advantages, they have certain problems. For example, they can produce different solutions with each execution; the solutions obtained may not guarantee global optimality; and they require a greater computational burden. However, it should be noted that these solutions are still valuable, efficient, and practical [30].

In evolutionary algorithms, parameter selection is crucial for optimal performance. For example, the PSO algorithm's key

parameters are population size, number of iterations, inertia weight, and cognitive and social learning factors. The population size influences exploration and exploitation trade-offs, while the number of iterations balances solution space exploration and computational efficiency. The inertia weight impacts exploration and exploitation tendencies, and cognitive and social learning factors regulate individual learning and swarm cooperation. Optimal parameter values significantly impact convergence speed, solution diversity, and the ability to find well-distributed Pareto optimal solutions [31].

Some base evolutionary algorithms, such as PSO, GA, and GWO, are effectively extended to handle problems with several objective functions. One of these algorithms is the MOPSO, which was introduced in 2004 by Coello Coello *et al.* [32]. Another algorithm is the NSGA-II, developed in 2002 by Kalyanmoy Deb *et al.* [33]. The MOGWO is another recently extended multi-objective algorithm introduced in 2016 by Seyedali Mirjalili *et al.* [34]. These algorithms obtained three sets of Pareto front solutions, which can be further evaluated to examine the results.

4. PROPOSED APPROACH

Detailed descriptions of the objective functions, constraints, and the proposed method are provided in this section.

4.1. Objective functions

The first objective function: The expected active power losses under the distribution network's normal operating situation are considered the first objective function, formulated as Eqs. (14) and (15).

$$F_1 = E\left[Plosses\right] = min(\sum_{k=1}^{K} P\left(X_k\right) \times Plosses\left(X_k\right)) \tag{14}$$

$$Plosses = \sum_{l=1}^{NL} G_l \left[V_i^2 + V_j^2 - 2\left|V_i\right|\left|V_j\right|\cos\left(\theta_i - \theta_j\right)\right] \tag{15}$$

where

G_l is the conductance of the line l between i and j buses;

V_i *and* V_j are voltages of the i and j buses;

θ_i *and* θ_j are voltage angles of the i and j buses;

NL is the number of distribution network feeders;

$Plosses\left(X_k\right)$ is the total active power losses with RES allocation based on the X_k input variables.

The second objective function: One of the objectives is to minimize the expected power not served. The EPNS is a suitable indicator for evaluating power system reliability [35]. The proposed reliability index considers the amount of power not served throughout all possible distribution line outages. Small values of the EPNS indicate that the power system is operating at a higher level of safety. Each contingency will cause a partial disconnection of the distribution network and result in PNS.

$$F_2 = E\left[PNS\right] = min(\sum_{k=1}^{K} P\left(X_k\right) \times PNS\left(X_k\right)) \tag{16}$$

$$PNS = \sum_{c=1}^{N_c} PNS_c \times \pi_c \tag{17}$$

where

c is a contingency index;

N_c indicates the number of contingency situations (feeder outages);

PNS_c is the amount of PNS throughout c^{th} contingency situation;

$PNS\left(X_k\right)$ is the k^{th} value of the PNS based on the X_k input variables;

π_c indicates the possibility of the c^{th} contingency situation computed as Eq. (18) [36].

$$\pi_c = PF \times \left(1 - PF\right)^{NB_c} \tag{18}$$

where

NB_c is the number of grid-connected feeders at c^{th} contingency situation;

PF is the probability of a single feeder outage.

The third objective function: A confidence interval estimates a parameter in a probabilistic environment. The width of the confidence interval is affected by many factors, including the confidence level, the sample size, and the variability of the sample. Confidence intervals are calculated at a specified level of confidence; the most common level is 95%. Confidence intervals at a given confidence level have a theoretical probability of containing the parameter's true value in the long run. A 95% confidence interval should contain 95% of the true value of the parameter [37]. The 95% confidence interval of a variable (X) can be calculated as Eqs. (19) and (20).

$$pr_X(a < X < b) = 95 \tag{19}$$

$$CI_X = b - a \tag{20}$$

The 95% confidence interval of the active power losses under the normal operating situation of the distribution network is considered the third objective function according to Eq. (21).

$$F_3 = min(CI_{Plosses}) \tag{21}$$

where $CI_{Plosses}$ indicates the 95% confidence interval of the active power losses; and can be calculated based on Eqs. (19) and (20). The power losses' confidence interval may differ from its expected value. According to Fig. 2, the expected values of power losses are the same but have different confidence interval values $(CI_1 > CI_2)$.

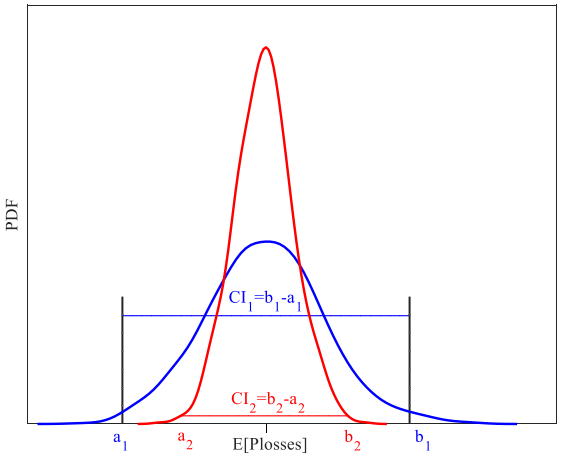

Fig. 2. Confidence interval values in different PDFs.

4.2. Constraints

Some constraints are associated with the RES allocation in the distribution network [38]. Constraint Eq. (22) is defined to keep the voltage of the bus within the allowed voltage range. It is necessary to limit the lines' current to protect the cables against high currents. Constraint Eq. (23) specifies the current limit for the lines.

$$V_i^{min} \leq V_i \leq V_i^{max} \tag{22}$$

$$I_b \leq I_b^{max} \tag{23}$$

where

V_i^{min} and V_i^{max} are the minimum and maximum voltage limits of the i^{th} bus;

V_i indicates the voltage of the i^{th} bus;

I_b^{max} is the maximum current limit of the b^{th} distribution line;

I_b indicates the current of the b^{th} distribution line.

4.3. Problem-solving

The flowchart of the problem-solving is illustrated in Fig. 3. According to the flowchart, network data should be input first. In the next step, three algorithms, i.e., MOPSO, NSGA II, and MOGWO, are used to determine the defined control variables, given in Eq. (24).

$$\text{Location}_{\text{RES}_1}.\ \text{Location}_{\text{RES}_2}.\ \ldots.\ \text{Location}_{\text{RES}_\text{d}} \tag{24}$$

$Location_{RES_1}.\ Location_{RES_2}.\ and\ Location_{RES_d}$ are respectively the bus numbers of the distribution network for allocating the $RES_1, RES_2, and\ RES_d$.

A matrix of uncertain variables is generated based on the PDFs outlined in Eqs. (1), (3), and (5). Instead of analyzing a large volume of data generated through MCS, data clustering methods facilitate the analysis of a finite number of datasets. Thus, the K-medoids data clustering method reduces the sample matrix to K clusters for N uncertain variables, such as load and RESs. In addition, the active power outputs of the RESs are calculated using wind speed and solar radiation samples, as defined in Eqs. (2), (4).

Subsequently, the PNS values for each dataset are derived using Eq. (17), considering all distribution line outages. By conducting a forward/backward load flow based on the acquired dataset, the active power losses under normal operating scenarios of the distribution network are calculated for each dataset. Based on the probability of each dataset, the expected values of the active power losses and PNS are determined using Eqs. (14) and (16), respectively. Furthermore, the confidence intervals of the active power losses are calculated utilizing the values of the active power losses of all K datasets.

Upon completing the defined populations and the number of iterations, algorithms optimize the defined problem and extract Pareto-based solutions. These solutions are analyzed, and the most appropriate and practical result is determined based on the considered criteria. Therefore, the TOPSIS, as a multi-criteria decision-making technique, is employed to select a final solution based on the defined weight coefficients of the objective functions [39].

5. Discussion and Simulation Results

In this research, the IEEE 33-bus and 118-bus distribution networks have been chosen as the case study to demonstrate the effectiveness of the proposed approach. So far, these networks have been extensively used for distribution network studies.

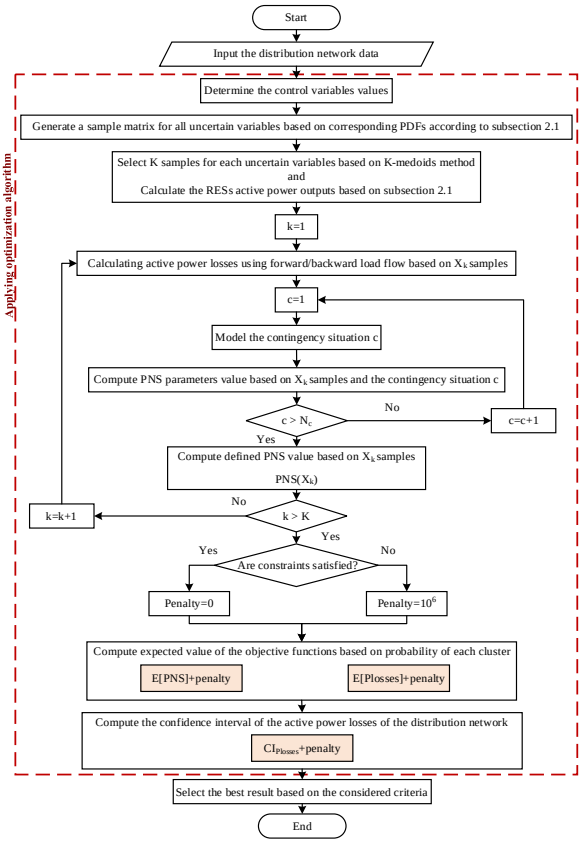

Fig. 3. The problem-solving flowchart.

Table 2. The related parameters of the WTs and PVs.

Units	Parameter	Value
WT	v^{cut-in}	3 (m/s)
	$v^{cut-out}$	25 (m/s)
	v^{rated}	13 (m/s)
PV	r^{cer}	0.15 (kW/m^2)
	r^{std}	1 (kW/m^2)

5.1. Assumptions

The RESs utilized in this study are WT and PV units with a stochastic output. WT's power generation is related to wind speed, and the behavior of wind speeds can be modeled using the Weibull distribution. The Weibull distribution parameters k and λ are equal to 3 and 8, respectively [40]. The PV's power generation is related to solar radiation, and the beta distribution can be used to model solar radiation. The beta distribution parameters α and β are 0.5 kW/m^2 and 0.3 kW/m^2, respectively [41]. The rest of the relevant data for WTs and PVs are presented in Table 2 [4].

Load power demand is modeled by the normal distribution. It is assumed that the base active power value represents the expected value of the loads. Moreover, the standard deviations of the loads are assumed to be 10% of their expected values [42]. The probability of the single feeder outage is assumed to be 0.01. Initially, 10,000 samples are generated for each uncertain input parameter by the MCS technique, which is subsequently reduced to 10 datasets through the K-medoids data clustering technique.

The MOPSO algorithm is set to have a population size of 100, 200 iterations, a repository size of 15, an inertia weight of 0.73, a cognitive learning factor of 1.49, and a social learning factor of 1.49. The MOGWO algorithm is set to have a population size of 100, 200 iterations, and a repository size of 15. On the other hand, the NSGA-II algorithm is configured with a generation size of 15,

Table 3. Optimal values of the objective functions in the 33-bus distribution network using MOPSO, NSGA II, and MOGWO algorithms.

	EPNS (kW)			Plosses (kW)			$CI_{Plosses}$ (kW)		
Solution	MOPSO	NSGA II	MOGWO	MOPSO	NSGA II	MOGWO	MOPSO	NSGA II	MOGWO
1	195.45	177.29	177.51	197.36	162.29	163.23	64.41	81.87	107.12
2	192.05	191.59	178.65	196.36	192.85	166.05	64.66	65.84	102.82
3	196.74	189.67	211.38	204.83	186.18	227.78	64.22	67.47	79.49
4	194.66	186.55	177.51	196.76	179.62	166.31	64.54	70.16	101.29
5	190.79	182.67	200.89	184.80	167.52	207.93	67.59	78.69	84.25
6	190.50	188.10	180.39	192.78	182.88	168.30	65.67	68.68	100.53
7	176.63	182.08	198.95	165.59	177.79	215.46	74.89	72.66	80.49
8	175.33	183.61	206.93	163.85	171.78	229.53	75.65	74.64	78.17
9	173.97	187.63	207.07	161.87	175.84	229.46	76.61	72.99	78.55
10	177.85	181.51	178.85	172.47	165.76	173.05	72.45	79.42	90.86
11	177.49	178.94	179.37	172.98	162.59	172.22	71.05	81.70	93.49
12	180.22	186.29	192.36	177.07	174.69	194.24	70.77	73.70	88.24
13	187.42	184.72	184.52	183.23	173.59	184.07	70.63	74.26	89.11
14	174.82	179.51	198.18	161.15	163.47	208.48	78.62	81.31	83.66
15	174.15	180.06	200.89	161.37	164.63	207.93	77.63	80.63	84.25

200 iterations, the size of the mating pool of 7, and a tournament size of 2.

5.2. The 33-bus distribution network

This network's total active and reactive loads are 3.715 MW and 2.3 MVAr, respectively, and the voltage rating is 12.66 kV. The highest voltage drop and increase within the system are 8.7% and 5%, respectively, while the maximum current capacity for the system branches is 255 A. The information regarding this network is fully available in reference [43], and its diagram is illustrated in Fig. 4.

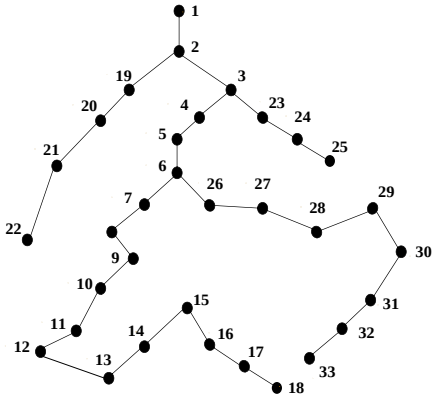

Fig. 4. The IEEE 33-bus test distribution network diagram.

The histograms of the demand load at bus 27, wind speed, and solar radiation samples are depicted in Figs. 5-(a), 5-(b), and 5-(c), respectively.

This study utilizes five RESs with various capacities to improve the proposed objectives. Three WT units with active power ratings equal to 250 kW, 200 kW, and 350 kW and two PV units with active power ratings equal to 200 kW and 100 kW are considered to be allocated to the distribution network. Fig. 6 indicates the initial and obtained solution points consisting of the EPNS, active power losses, and $CI_{Plosses}$ in the objective area. This figure shows the initial points in green stars and Pareto front solutions of the MOPSO, NSGA II, and MOGWO optimization algorithms in black, red, and blue stars, respectively.

The data presented in Fig. 6 could assist the system operator in making decisions from various points of view. The optimal values of the objective functions related to the solution points of Fig. 6 are presented in Table 3.

According to Fig. 6 and the data presented in Table 3, the EPNS variations are 13.09%, 8.06%, and 19.08%; the Plosses variations are 27.10%, 18.83%, 40.61%; and $CI_{Plosses}$ variations are 19.29%, 24.34%, and 37.03% using MOPSO, NSGA II, and MOGWO algorithms, respectively. Obviously, these objective functions have wide variations; employing a selecting approach

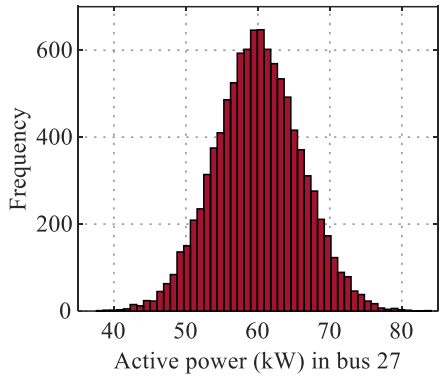

(a)

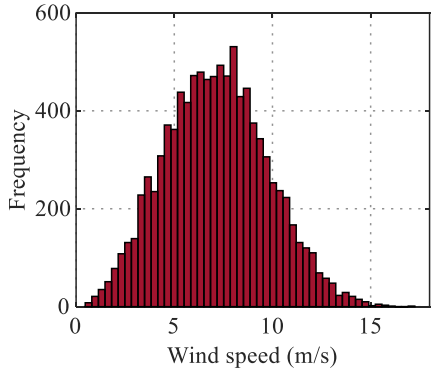

(b)

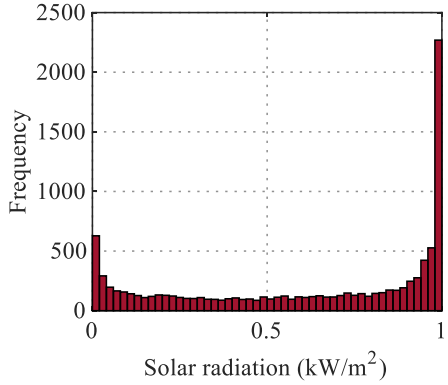

(c)

Fig. 5. The corresponding histograms of the demand load at bus 27, wind speed, and solar radiation samples.

is vital; and the decision-maker must consider the conflict of the objectives.

In this regard, the TOPSIS technique as a multi-criteria approach is used to select a solution in the MOPSO algorithm, and the selected solution is compared with a solution in NAGA II and MOGWO algorithms that have similar EPNS and Plosses values. The $CI_{Plosses}$ value in different Pareto front solutions can be compared in this strategy. Additionally, this method effectively demonstrates the fluctuations in $CI_{Plosses}$ with the equivalent values of EPNS and Plosses in different algorithms. By defining the similar weight coefficients for the objective function as

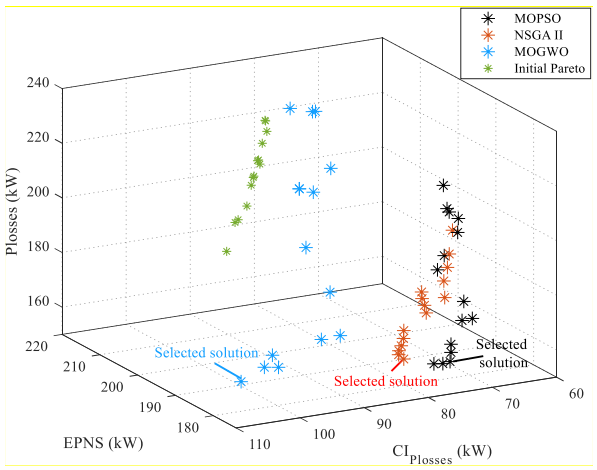

Fig. 6. The initial and obtained Pareto front solutions of the 33-bus distribution network using MOPSO, NSGA II, and MOGWO algorithms.

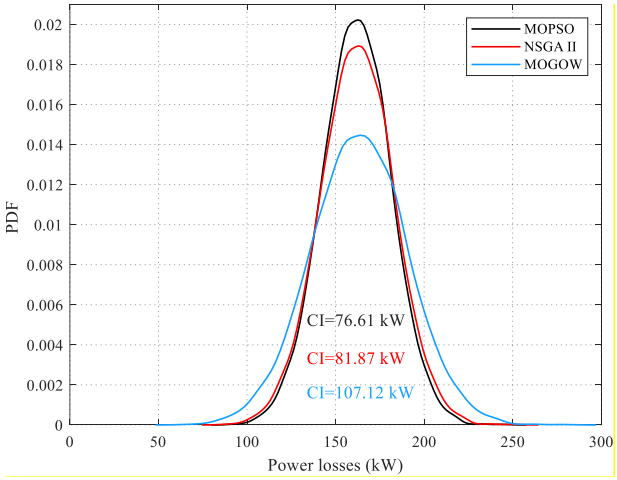

Fig. 7. The PDF representation of active power losses in selected solutions of the MOPSO, NSGA II, and MOGWO algorithms in the 33-bus distribution network.

$\omega_{EPNS} = 0.33$, $\omega_{Plosses} = 0.33$, and $\omega_{CI} = 0.33$, a solution from the MOPSO solutions is selected.

As depicted in Fig. 6 and according to the data presented in Table 3, Solution 9 from MOPSO and Solution 1 from both the NSGA II and MOGWO optimization algorithms have been selected to evaluate and compare the results obtained from the respective Pareto solutions. The EPNS values are 173.97 kW, 177.29 kW, and 177.51 kW, and the Plosses values are 161.87 kW, 162.29 kW, and 163.23 kW in the MOPSO, NSGA II, and MOGWO algorithms, respectively. The EPNS and Plosses values obtained from the three algorithms are close to each other. Consequently, the $CI_{Plosses}$ index is crucial in this situation due to its variability. The $CI_{Plosses}$ values are 76.61 kW, 81.87 kW, and 107.12 kW in the MOPSO, NSGA II, and MOGWO algorithms, respectively. The $CI_{Plosses}$ value in Solution 9 of the MOPSO algorithm is 39.82% and 6.86% lower than the $CI_{Plosses}$ value in the selected solution of the NSGA II and MOGWO algorithms, respectively. Based on these findings, Fig. 7 illustrates the active power losses for the three selected solutions in PDF format to show the 95% $CI_{Plosses}$ effect on the power losses.

As illustrated in Fig. 7, the $CI_{Plosses}$ value in the MOPSO algorithm causes a narrow PDF representation. Solutions with a smaller $CI_{Plosses}$ value provide higher levels of certainty,

Table 4. Optimal locations of WT and PV units in the 33-bus distribution network based on the selected solutions of the MOPSO, NSGA II, and MOGWO algorithms.

	Location				
Selected solution	WT1	WT2	WT3	PV1	PV2
Solution 8 in the MOPSO algorithm	16	17	18	31	32
Solution 1 in the NSGA II algorithm	18	14	33	16	9
Solution 1 in the MOGWO algorithm	32	16	18	33	15

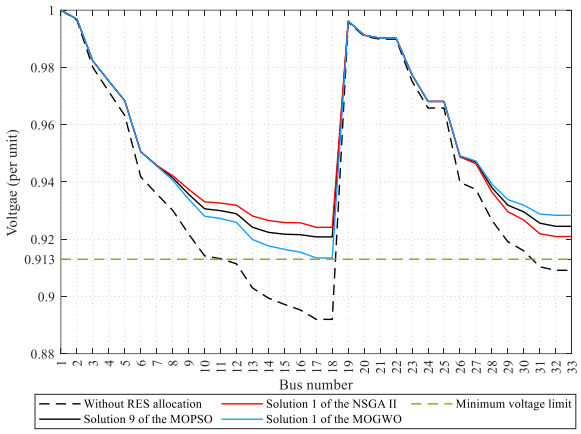

Fig. 8. Voltage profiles of the 33-bus distribution network.

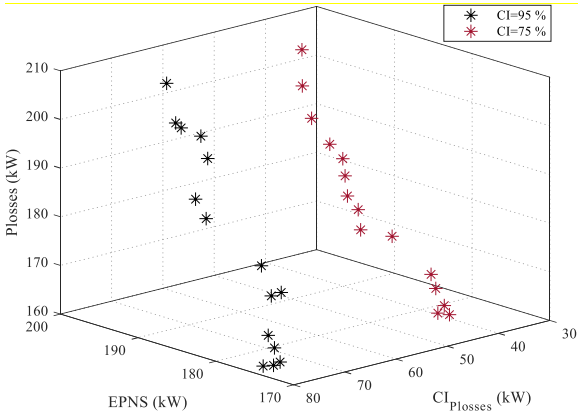

Fig. 9. The pareto front solutions obtained with 75% and 95% confidence intervals of the power losses using the MOPSO algorithm.

resulting in more accurate decision-making in power systems. This strategy involves allocating RESs to the network with reasonable levels of $CI_{Plosses}$ and considering similar values of active power losses shown in Fig. 7. Table 4 provides the determined control variables in the selected solutions to present the WT and PV unit locations in the 33-bus distribution network.

Based on the results and discussions presented, applying the MOPSO optimization algorithm and selecting Solution 9 is more logical than other algorithms and solutions; besides, there is greater certainty in power losses while RESs are allocated to the 33-bus distribution network.

The voltage profiles of the 33-bus distribution network are illustrated in Fig. 8. This figure presents the voltage profile of the network without RES allocation and with optimal RES allocation based on selected solutions and specifies the minimum voltage limit.

Based on the presented figure, the network voltage has been violated without RES allocation in some buses; however, the voltage limit is satisfied with RES allocation. Moreover, voltage profiles based on the selected optimal solutions of the MOPSO and

Table 5. Optimal values of the objective functions in the 118-bus distribution network using MOPSO, NSGA II, and MOGWO algorithms.

	EPNS (kW)			Plosses (kW)			$CI_{Plosses}$ (kW)		
Solution	MOPSO	NSGA II	MOGWO	MOPSO	NSGA II	MOGWO	MOPSO	NSGA II	MOGWO
1	498.72	491.01	503.09	1044.13	1006.71	1201.06	112.41	187.57	250.36
2	513.84	511.38	527.00	1008.53	950.78	912.57	122.52	115.04	202.84
3	527.88	532.62	521.12	1006.41	1036.96	991.53	100.56	73.08	117.45
4	531.22	502.89	518.93	969.23	1088.58	1079.55	97.58	128.87	129.50
5	533.30	519.53	512.11	947.37	980.63	953.02	88.33	106.41	114.96
6	524.52	528.18	504.36	910.39	1004.11	1172.39	120.58	88.79	156.58
7	533.08	523.69	509.73	969.34	984.67	1147.73	96.25	102.72	143.62
8	522.27	497.91	516.54	930.99	1044.34	1035.69	112.39	167.95	157.47
9	515.83	508.05	517.21	1003.68	1037.94	967.43	148.83	177.76	199.04
10	518.33	509.88	513.58	944.75	1070.67	1011.74	117.90	157.24	227.56
11	525.76	509.07	508.21	942.08	1097.82	1090.82	108.61	127.76	150.28
12	528.68	531.76	510.67	934.37	1012.36	1052.26	107.23	82.28	244.27
13	516.78	505.06	519.49	910.97	959.05	1005.17	141.53	194.63	164.07
14	527.35	506.87	522.03	940.29	974.22	996.04	102.73	179.53	92.75
15	520.21	521.24	514.75	909.90	970.62	1069.97	122.79	104.98	133.93

Table 6. Optimal locations of WT and PV units in the 118-bus distribution network based on the selected solutions of the MOPSO, NSGA II, and MOGWO algorithms.

	Location									
Selected solution	WT1	WT2	WT3	WT4	WT5	PV1	PV2	PV3	PV4	PV5
Solution 5 in the MOPSO algorithm	72	47	94	70	32	111	99	73	67	77
Solution 2 in the NSGA II algorithm	110	91	53	76	27	111	112	97	35	75
Solution 2 in the MOGWO algorithm	79	53	112	71	75	73	68	32	70	97

NSGA II algorithms are better than MOGWO. Another scenario is defined to investigate the effect of confidence interval level on the problem outputs. In this scenario, the same strategy with a 75% confidence interval of the power losses is defined, and a set of Pareto front solutions is obtained using the MOPSO algorithm. Fig. 9 illustrates these solutions and the previously obtained results using the MOPSO algorithm.

Based on this figure, changing the confidence interval level does not affect the output results, and the EPNS and Plosses values are similar to each other. This figure proves the generality of the proposed strategy.

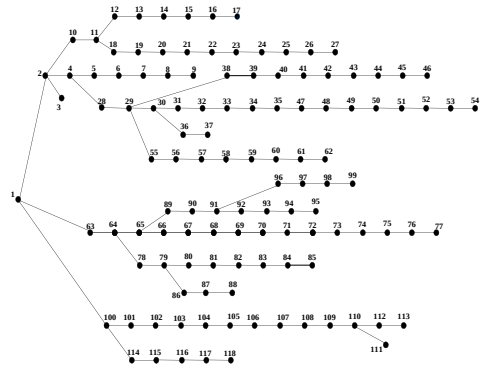

Fig. 10. The IEEE 118-bus test distribution network diagram.

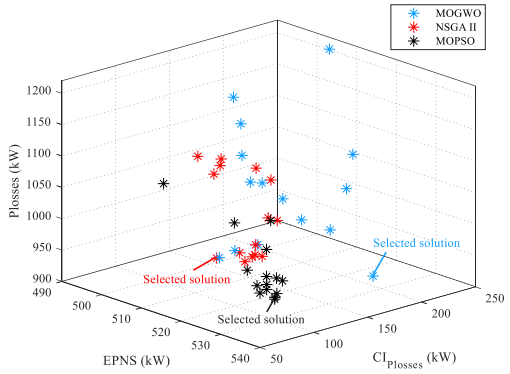

Fig. 11. The obtained Pareto front solutions of the 118-bus distribution network using MOPSO, NSGA II, and MOGWO algorithms.

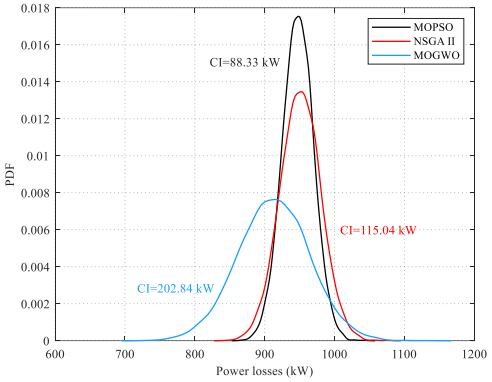

Fig. 12. The PDF representation of active power losses in the selected solutions of MOPSO, NSGA II, and MOGWO algorithms in the 118-bus distribution network.

5.3. The 118-bus distribution network

The IEEE 118-bus distribution network is a large-scale study system including 117 buses and 118 branches, with total active and reactive loads of 22,709.72 kW and 17041.07 kVAr, respectively. The test system's power and voltage base values are 100 MVA and 11 kV, respectively. System data are taken from [44] and its diagram is illustrated in Fig. 10.

equal to 750 kW, 500 kW, 400, 500, and 350 kW to be allocated to the distribution network. Fig. 11 indicates the obtained solution points consisting of the EPNS, active power losses, and $CI_{Plosses}$ in the objective area. Table 5 lists the optimal values of the objective functions related to the solution points of Fig. 11.

According to Fig. 11 and the data in Table 5, the EPNS variations are 6.93%, 8.47%, and 4.75%; the Plosses variations are 14.750%, 14.46%, 31.61%; and $CI_{Plosses}$ variations are 68.49%, 127.96%, and 169.92% using MOPSO, NSGA II, and MOGWO algorithms, respectively. The $CI_{Plosses}$ have wide variations in the 118-bus distribution and an approach that considers the conflict of this index with other objectives must be adopted.

By defining the similar weight coefficients for the objective function as $\omega_{EPNS} = 0.33$, $\omega_{Plosses} = 0.33$, and $\omega_{CI} = 0.33$, Solution 5 of the MOPSO solutions is selected. In this solution, the EPNS, Plosses, and $CI_{Plosses}$ values are 533.30 kW, 947.37 kW, and 88.33 kW, respectively. Solution 2 from both the NSGA II and MOGWO optimization algorithms has been selected to evaluate and compare the results obtained from the respective Pareto solutions. The EPNS and Plosses values derived from the three algorithms are similar to each other, and the $CI_{Plosses}$ values are 88.33 kW, 115.04 kW, and 202.84 kW in the MOPSO, NSGA II, and MOGWO algorithms, respectively.

The $CI_{Plosses}$ value in Solution 5 of the MOPSO algorithm is 129.63% and 30.23% lower than the selected solution of the NSGA II and MOGWO algorithms, respectively. Based on these findings, Fig. 12 depicts the active power losses for three selected solutions in PDF format to show the 95% $CI_{Plosses}$ effect on the power losses.

As displayed in Fig. 12, the $CI_{Plosses}$ value in the MOPSO algorithm has a narrow PDF profile. This selected solution has a smaller $CI_{Plosses}$ value, which provides higher levels of certainty and results in more accurate decision-making in power systems. This strategy involves allocating RESs to the network with reasonable levels of $CI_{Plosses}$ and considering similar values of active power losses. Table 6 provides the determined control variables in the selected solutions to present the WT and PV unit locations in the 118-bus distribution network.

Based on the results and discussions presented, applying the MOPSO optimization algorithm and selecting Solution 5 is more logical than the other algorithms and solutions.

6. CONCLUSION

This paper proposed a robust scheme for optimal locations of RESs in 33-bus and 118-bus distribution networks, by considering the confidence interval concept. The proposed optimization problem was solved in a multi-objective framework in which the objectives were the EPNS reliability index in contingency situations, active power losses under normal operating situations, and a confidence interval of power losses. The K-medoids data clustering method was employed to manage the uncertainty of RESs and demand loads as an effective uncertainty modeling technique. The MOPSO, NSGA II, and MOGWO algorithms were used as the optimization tools. In addition, the TOPSIS technique was utilized to select the final solutions among the optimized solutions. The proposed technique could help operators to select a proper solution to make more reliable and valid decisions.

The obtained results show that without needing to increase the EPNS and losses, the confidence interval can be increased, considerably. In the 33-bus distribution network, with similar values of the EPNS and Plosses, the $CI_{Plosses}$ value in the selected solution of the MOPSO algorithm was 6.86% and 39.82% lower than the NSGA II and MOGWO algorithms, respectively. Similarly, in the 118-distribution network, the $CI_{Plosses}$ value in the selected solution of the MOPSO algorithm was 30.23% and 129.63% less than the NSGA II and MOGWO algorithms, respectively. This comparative analysis demonstrated the superior performance of the MOPSO algorithm in minimizing $CI_{Plosses}$ in both the 33- and 118-bus distribution networks, which increases the certainty of the predicted value of the power losses. Based on the discussions by applying the MOPSO optimization algorithm, a solution is selected with EPNS, Plosses, and $CI_{Plosses}$ values of 173.97 kW, 161.87 kW, and 76.61 kW for the 33-bus distribution network, and 533.30 kW, 947.37 kW, and 88.33 kW for the 118-bus distribution network.

Looking ahead, future research can focus on the following research areas:

- Optimal planning of RESs considering the dependence of various non-technical and market policies in addition to economic and technical objectives
- Optimal planning of RESs with energy storage systems presence
- Considering the correlations among the stochastic variables
- Investigating the effect of confidence interval decreasing from the cost aspect

REFERENCES

[1] Y. Gilasi, S. H. Hosseini, and H. Ranjbar, "Resiliency-oriented optimal siting and sizing of distributed energy resources in distribution systems," *Electr. Power Syst. Res.*, vol. 208, p. 107875, 2022.

[2] A. Younesi, H. Shayeghi, P. Siano, and A. Safari, "A multi-objective resilience-economic stochastic scheduling method for microgrid," *Int. J. Electr. Power Energy Syst.*, vol. 131, p. 106974, 2021.

[3] P. Meera and S. Hemamalini, "Reliability assessment and enhancement of distribution networks integrated with renewable distributed generators: A review," *Sustainable Energy Technol. Assess.*, vol. 54, p. 102812, 2022.

[4] H. Ebrahimi, S. Galvani, V. Talavat, and M. Farhadi-Kangarlu, "A conditional value at risk based stochastic allocation of sop in distribution networks," *Electr. Power Syst. Res.*, vol. 228, p. 110111, 2024.

[5] Y. Luo, Q. Nie, D. Yang, and B. Zhou, "Robust optimal operation of active distribution network based on minimum confidence interval of distributed energy beta distribution," *J. Mod. Power Syst. Clean Energy*, vol. 9, no. 2, pp. 423–430, 2020.

[6] T. E. Gümüş, S. Emiroglu, and M. A. Yalcin, "Optimal dg allocation and sizing in distribution systems with thevenin based impedance stability index," *Int. J. Electr. Power Energy Syst.*, vol. 144, p. 108555, 2023.

[7] K. Subbaramaiah, P. Sujatha, *et al.*, "Optimal dg unit placement in distribution networks by multi-objective whale optimization algorithm & its techno-economic analysis," *Electr. Power Syst. Res.*, vol. 214, p. 108869, 2023.

[8] S. Abdul-Ameer, A. Al-Nussairi, R. Khalid, J. Abbas, and A. Al-Mansor, "Maximizing the generated power of wind farms by using optimization method," *J. Oper. Autom. Power Eng.*, vol. 11, no. Special Issue (Open), 2023.

[9] A. Selim, S. Kamel, and F. Jurado, "Efficient optimization technique for multiple dg allocation in distribution networks," *Appl. Soft Comput.*, vol. 86, p. 105938, 2020.

[10] L. A. Gallego Pareja, J. M. López-Lezama, and O. Gómez Carmona, "Optimal feeder reconfiguration and placement of voltage regulators in electrical distribution networks using a linear mathematical model," *Sustainability*, vol. 15, no. 1, p. 854, 2023.

[11] M. Dixit, P. Kundu, and H. R. Jariwala, "Integration of distributed generation for assessment of distribution system reliability considering power loss, voltage stability and voltage deviation," *Energy Syst.*, vol. 10, pp. 489–515, 2019.

[12] R. Fathi, B. Tousi, and S. Galvani, "Allocation of renewable resources with radial distribution network reconfiguration using improved salp swarm algorithm," *Appl. Soft Comput.*, vol. 132, p. 109828, 2023.

[13] S. Rezaeian-Marjani, S. M. Jalalat, B. Tousi, S. Galvani, and V. Talavat, "A probabilistic approach for optimal operation of wind-integrated power systems including upfc," *IET Renewable Power Gener.*, vol. 17, no. 3, pp. 706–724, 2023.

[14] L. C. da Costa, F. S. Thomé, J. D. Garcia, and M. V. Pereira, "Reliability-constrained power system expansion planning: A stochastic risk-averse optimization approach," *IEEE Trans. Power Syst.*, vol. 36, no. 1, pp. 97–106, 2020.

[15] H. Ebrahimi, S. Rezaeian-Marjani, S. Galvani, and V. Talavat, "Probabilistic optimal planning in active distribution networks considering non-linear loads based on data clustering method," *IET Gener. Transm. Distrib.*, vol. 16, no. 4, pp. 686–702, 2022.

[16] L. A. Gallego, J. F. Franco, and L. G. Cordero, "A fast-specialized point estimate method for the probabilistic optimal power flow in distribution systems with renewable distributed generation," *Int. J. Electr. Power Energy Syst.*, vol. 131, p. 107049, 2021.

[17] J. S. Giraldo, J. C. López, J. A. Castrillon, M. J. Rider, and C. A. Castro, "Probabilistic opf model for unbalanced three-phase electrical distribution systems considering robust constraints," *IEEE Trans. Power Syst.*, vol. 34, no. 5, pp. 3443–3454, 2019.

[18] L. G. C. Bautista, J. Soares, J. F. F. Baquero, and Z. Vale, "Probabilistic algorithm based on 2m+ 1 point estimate method edgeworth considering voltage confidence intervals for optimal pv generation," in *2022 17th Int. Conf. Probab. Methods Appl. Power Syst. (PMAPS)*, pp. 1–6, IEEE, 2022.

[19] S. Zhang, H. Cheng, K. Li, N. Tai, D. Wang, and F. Li, "Multi-objective distributed generation planning in distribution network considering correlations among uncertainties," *Appl. Energy*, vol. 226, pp. 743–755, 2018.

[20] H.-S. Park and C.-H. Jun, "A simple and fast algorithm for k-medoids clustering," *Expert Syst. Appl.*, vol. 36, no. 2, pp. 3336–3341, 2009.

[21] C. Wang, C. Liu, F. Tang, D. Liu, and Y. Zhou, "A scenario-based analytical method for probabilistic load flow analysis," *Electr. Power Syst. Res.*, vol. 181, p. 106193, 2020.

[22] M. D. McKay, R. J. Beckman, and W. J. Conover, "A comparison of three methods for selecting values of input variables in the analysis of output from a computer code," *Technometrics*, vol. 42, no. 1, pp. 55–61, 2000.

[23] M. Vahid-Pakdel and B. Mohammadi-Ivatloo, "Probabilistic assessment of wind turbine impact on distribution networks

using linearized power flow formulation," *Electr. Power Syst. Res.*, vol. 162, pp. 109–117, 2018.

[24] M. Aien, M. Fotuhi-Firuzabad, and M. Rashidinejad, "Probabilistic optimal power flow in correlated hybrid wind–photovoltaic power systems," *IEEE Trans. Smart Grid*, vol. 5, no. 1, pp. 130–138, 2014.

[25] M. Kumar and C. Samuel, "Statistical analysis of load demand distribution at banaras hindu university, india," in *2016 Int. Conf. Adv. Comput. Commun. Inf. (ICACCI)*, pp. 2318–2323, IEEE, 2016.

[26] S. Rezaeian-Marjani, S. Galvani, V. Talavat, and M. Farhadi-Kangarlu, "Optimal allocation of d-statcom in distribution networks including correlated renewable energy sources," *Int. J. Electr. Power Energy Syst.*, vol. 122, p. 106178, 2020.

[27] R. Xu and D. Wunsch, "Survey of clustering algorithms," *IEEE Trans. Neural Networks*, vol. 16, no. 3, pp. 645–678, 2005.

[28] L. Kaufman and P. J. Rousseeuw, *Finding groups in data: an introduction to cluster analysis*. John Wiley & Sons, 2009.

[29] R. Avvari and V. K. DM, "A novel hybrid multi-objective evolutionary algorithm for optimal power flow in wind, pv, and pev systems," *J. Oper. Autom. Power Eng.*, vol. 11, no. 2, pp. 130–143, 2023.

[30] S. Galvani, A. Bagheri, M. Farhadi-Kangarlu, and N. Nikdel, "A multi-objective probabilistic approach for smart voltage control in wind-energy integrated networks considering correlated parameters," *Sustainable Cities Soc.*, vol. 78, p. 103651, 2022.

[31] Y. He, W. J. Ma, and J. P. Zhang, "The parameters selection of pso algorithm influencing on performance of fault diagnosis," in *MATEC Web Conf.*, vol. 63, p. 02019, EDP Sciences, 2016.

[32] C. A. C. Coello, G. T. Pulido, and M. S. Lechuga, "Handling multiple objectives with particle swarm optimization," *IEEE Trans. Evol. Comput.*, vol. 8, no. 3, pp. 256–279, 2004.

[33] K. Deb, A. Pratap, S. Agarwal, and T. Meyarivan, "A fast and elitist multiobjective genetic algorithm: Nsga-ii," *IEEE Trans. Evol. Comput.*, vol. 6, no. 2, pp. 182–197, 2002.

[34] S. Mirjalili, S. Saremi, S. M. Mirjalili, and L. d. S. Coelho, "Multi-objective grey wolf optimizer: a novel algorithm for multi-criterion optimization," *Expert Syst. Appl.*, vol. 47, pp. 106–119, 2016.

[35] J. Juan and I. Ortega, "Reliability analysis for hydrothermal generating systems including the effect of maintenance scheduling," *IEEE Trans. Power Syst.*, vol. 12, no. 4, pp. 1561–1568, 1997.

[36] S. Galvani, V. Talavat, and S. Rezaeian Marjani, "Preventive/corrective security constrained optimal power flow using a multiobjective genetic algorithm," *IEEE Trans. Power Syst.*, vol. 46, no. 13, pp. 1462–1477, 2018.

[37] F. D. C. Kraaikamp and H. L. L. Meester, "A modern introduction to probability and statistics," *Springer: Berlin/Heidelberg, Germany*, 2005.

[38] H. Ebrahimi, S. Galvani, V. Talavat, and M. Farhadi-Kangarlu, "Optimal parameters setting for soft open point to improve power quality indices in unbalanced distribution systems considering loads and renewable energy sources uncertainty," *Electr. Power Syst. Res.*, vol. 229, p. 110155, 2024.

[39] H. Ebrahimi, S. R. Marjani, and V. Talavat, "Optimal planning in active distribution networks considering nonlinear loads using the mopso algorithm in the topsis framework," *Int. Trans. Electr. Energy Syst.*, vol. 30, no. 3, p. e12244, 2020.

[40] H. Ebrahimi, S. Rezaeian-Marjani, M. Farhadi-Kangarlu, and S. Galvani, "Stochastic scheduling of energy storage systems in harmonic polluted active distribution networks," *IET Gener. Transm. Distrib.*, vol. 16, no. 23, pp. 4689–4709, 2022.

[41] M. Aien, M. Fotuhi-Firuzabad, and M. Rashidinejad, "Probabilistic optimal power flow in correlated hybrid wind–photovoltaic power systems," *IEEE Trans. Smart Grid*, vol. 5, no. 1, pp. 130–138, 2014.

[42] G. Carpinelli, R. Rizzo, P. Caramia, and P. Varilone, "Taguchi's method for probabilistic three-phase power flow of unbalanced distribution systems with correlated wind and photovoltaic generation systems," *Renewable Energy*, vol. 117, pp. 227–241, 2018.

[43] M. E. Baran and F. F. Wu, "Network reconfiguration in distribution systems for loss reduction and load balancing," *IEEE Trans. Power Delivery*, vol. 4, no. 2, pp. 1401–1407, 1989.

[44] J. Zhou, B. Ayhan, C. Kwan, S. Liang, and W. Lee, "High performance arcing fault localization in distribution networks," in *2011 IEEE Ind. Appl. Soc. Annu. Meet.*, pp. 1–5, IEEE, 2011.